

Ignition Times for Thermally Thick and Intermediate Conditions in Flat and Cylindrical Geometries

Michael A. Delichatsios
Fire Science and Technology Laboratory
CSIRO - Div of Building Construction & Engineering
PO Box 310 North Ryde 1670
Australia

Abstract

Time to ignition data, usually in the presence of a pilot, for endothermically decomposing materials have been extensively measured over the last thirty years in cone calorimeter type apparatus where the material is exposed to external radiation heat fluxes in the range of 20 to 100 kW / m² in a horizontal orientation. These data have been used as a) a measure of ignitability and b) as a means to deduce material properties such as thermal inertia and critical heat flux. The approach to deduce these properties is based on conduction heat transfer without properly accounting for front or rear surface heat losses in conjunction to the thickness of the material. Thus severe confusion has been created in the fire field concerning the interpretation of ignition data. This paper delineates all the regimes for proper interpretation of ignition data so that reported inconsistencies can be explained. In the present case, the rear surface is insulated and the major contribution to heat losses is from surface radiation because the material is horizontal.

1. Introduction

Piloted ignition of solids occurs when their surface temperature reaches a value that usually corresponds to a characteristic pyrolysis temperature for the degradation of the material. This description is supported by experiments and also supported by asymptotic analysis for the pyrolysis process if the pyrolysis rate is approximated by an Arrhenius expression having high activation energy[1,2,3]. It follows that the time to ignition will be determined by the time required for the surface temperature to reach the so called ignition/ pyrolysis temperature. The ignition / pyrolysis temperature is high enough (more than 650 K) so that reradiation losses is the dominant heat loss mechanism from the surface which is horizontal in the typical cone type calorimeter tests . Ignition will not

occur, if the imposed heat flux is less than the surface reradiation loss at the ignition temperature, $\dot{q}_{cr}'' = \sigma T_{ign}^4$, which is also characterized as critical heat flux[1,2]. The ignition time can be determined from the response of the solid material to an imposed heat flux, as it is commonly done in flammability apparatus[1,2,3].

2. Problem Identification

There is considerable uncertainty in the literature about the appropriate way of plotting piloted ignition data as it is illustrated in Figure 1[1]. The authors of this paper (as well as others) use elements of conduction theory to plot ignition time data as the inverse square root of time (thermally thick) or the inverse time (thermally thin) versus the imposed radiant flux. When plotting piloted ignition data for 6 mm thick wood sample, the authors claim that both methods correlate the data well [1]. A problem arises when it is stated that the intercept for each method should be the critical heat flux , because the intercepts do not coincide (see Fig 1).

The present work points out to a clear way for correlating piloted ignition data with the objective of providing flammability properties needed to predict fire growth. Our approach is to examine first purely thermally thin situations (which have similar behavior for flat and cylindrical (cable) geometries) and then, thermally thick situations including intermediate cases(which have different behavior for flat and cylindrical geometries).

3. Thermally Thin Case

We consider physically thin materials (thickness or radius typically less than 1 mm) so that the sample behaves as thermally thin even for a high heat flux , \dot{q}'' , fixed during the test. Also, the back surface of the flat sample is insulated. The energy (heatup) equation for the sample uniform temperature is:

$$\rho c \delta \frac{dT}{dt} = \dot{q}'' - \sigma T^4 \quad (1)$$

where ρ is the density; c is the specific heat; δ is the thickness of the material ($\delta = r / 2$ for a cylindrical sample of radius r); σ is the Boltzmann constant and the emissivity of the surface is considered to be one (in some apparatus the surface is blackened by carbon black[2]). Finally, in Equ. 1 we neglect radiation from the ambient air as well as convective heat fluxes, both being negligible relative to the other energy terms.

We have obtained two asymptotic solutions for the thermally thin case:

$$\text{For } \dot{q}'' > 2\dot{q}_{cr}'' : T - T_o = \frac{t_{ign}}{\rho c \delta} (\dot{q}'' - \dot{q}_{int}'') \quad \text{where the intercept is } \dot{q}_{int}'' = .3\dot{q}_{cr}'' \quad (2a)$$

$$\text{For } \dot{q}'' < 1.2 \dot{q}_{cr}'' : \ln\left(\frac{\dot{q}'' - \dot{q}_{cr}''}{8\dot{q}_{cr}''}\right) = -\frac{4t_{ign}\dot{q}''}{\rho c \delta T^*} \quad \text{where } \dot{q}_{cr}'' = \sigma T_{ign}^4 \quad (2b)$$

These results are supported by “exact” numerical solutions of the partial differential heat transfer equation [4] as shown in Figure 2 (the agreement with Equation 2a is remarkable; the last point to the right deviates from thermally thin conditions). Equ 2a explains why the intercept of t^{-1} versus \dot{q}'' shown in Fig. 3 for a cable [5] is one third of the critical heat flux.

4. Thermally Thick Case

For the thermally infinite case, one can use the results of Panagiotou et. al.[3] which are:

$$\text{a. For } \dot{q}'' > 2\dot{q}_{cr}'' : \frac{1}{\sqrt{t_{ign}}} = \frac{2}{\sqrt{\pi}} \cdot \frac{\dot{q}'' - 64\dot{q}_{cr}''}{\sqrt{k\rho c(T_{ign} - T_o)}} \quad (3a)$$

$$\text{b. For } \dot{q}'' < 1.2 \dot{q}_{cr}'' : \frac{1}{\sqrt{t_{ign}}} = \frac{\pi}{\sqrt{\pi}} \cdot \frac{\dot{q}'' - \dot{q}_{cr}''}{\sqrt{k\rho c(T_{ign} - T_o)}} \quad (3b)$$

These results were derived by asymptotic analysis, verified by numerical analysis and compared with experiments [3]. Fig. 4a shows numerical calculations of $t_{ign}^{-1/2}$ versus \dot{q}'' for a 200mm thick PMMA sample plotted in normalized

coordinates: $\frac{\delta}{\sqrt{\alpha t_{ign}}}$ versus $\frac{\dot{q}'' \delta}{k(T_{ign} - T_o)}$, as suggested from simple conduction theory

[6]. The results, slopes and intercepts at high and low heat fluxes, are consistent with Eqs. 3a and 3b.

5. Finite Thickness Samples

For high imposed heat fluxes, the material behaves as thermally thick. This is supported by experiments (Fig.1) and numerical analysis. In Figures 4b and 4c we plot numerical results for different sample thickness (3, 5, 10, 20 mm) using the normalized coordinates

$\frac{\delta}{\sqrt{\alpha t_{ign}}}$ versus $\frac{\dot{q}'' \delta}{k(T_{ign} - T_o)}$. We distinguish two cases:

a) Reradiation losses are neglected. In this case all data fall on the same line, as classical conduction theory predicts (dashed line in Fig.4b). For large heat fluxes the material behaves as thermally thick ($t_{ign}^{-1/2}$ proportional to \dot{q}''), whereas for low heat it behaves as thermally thin (t_{ign}^{-1} proportional to \dot{q}'' which means that $t_{ign}^{-1/2}$ proportional to $\dot{q}''^{1/2}$). PMMA properties used here: $k = .23$ W/m K, $\rho = 1200$ kg/m³, $c = 2200$ J/kg K, $T_{ign} = 648$ K.

b) When reradiation losses are included the time to ignition data do not fall on the same line. We can notice that at high heat fluxes the sample behaves as thermally thick with

the same slope as when the reradiation losses are zero but displaced as if the imposed heat flux was $\dot{q}'' - 0.64 \dot{q}_{cr}''$, which again agrees with Equ 3a for thermally thick samples. This is also seen in Fig. 4c showing ignition time calculations for samples of thickness 20 and 200 mm. In this Figure the heat flux in the abscissa has been reduced by $0.64 \dot{q}_{cr}''$.

As the heat flux decreases, ignition times for various material thickness behave in a qualitatively different way relative to the asymptotic straight line corresponding to high heat fluxes (see Figures 4a, 4b and 4c). This difference in behavior for low heat fluxes is illustrated in Fig. 5 where it is shown that a) for thermally thick samples the ignition data fall below the asymptotic line, extrapolated to zero, b) for non-reradiation losses the ignition data fall above the asymptotic line, and c) for intermediate cases the ignition data behave in a mixed way. In addition, the numerical results in Fig. 4b indicate that up to 10 mm thick samples, ignition times in an intermediate heat flux regime (between 1.5 to 2 times the critical heat flux) are displaced parallel to the data for the no-reradiation loss case as if the heat flux is reduced by $0.64 \dot{q}_{cr}''$. Based on the present data in Figures

4a, 4b, and 4c , this intermediate regime will be present only when:
$$\frac{\dot{q}_{cr}'' \delta}{\sqrt{k\rho c(T_{ign} - T_o)}} < 1$$

(4)

In this regime an expression for the ignition time can be found by using solutions for the case without losses and incorporating the shift discussed prior to Equ. 4:

For Flat Samples

$$\frac{1}{\sqrt{t_{ign}}} = \frac{2}{\sqrt{\pi}} \cdot \frac{\dot{q}'' - .64\dot{q}_{cr}''}{\sqrt{k\rho c(T_{ign} - T_o)}} (1 + 2\sqrt{\pi} \left(\frac{1}{\sqrt{\pi}} e^{-\frac{\delta^2}{\alpha t}} - \sqrt{\frac{\delta^2}{\alpha t}} \operatorname{erfc}\left(\sqrt{\frac{\delta^2}{\alpha t}}\right) \right)) \quad (5a)$$

(Notice that for large heat fluxes the intercept is always shifted by $.64\dot{q}_{cr}''$, independently of material thickness)

For Cylindrical Samples

$$\frac{1}{\sqrt{t_{ign}}} = \frac{2}{\sqrt{\pi}} \cdot \frac{\dot{q}'' - .64\dot{q}_{cr}''}{\sqrt{k\rho c(T_{ign} - T_o)}} + \frac{\sqrt{\pi}}{4} \cdot \frac{\sqrt{\alpha}}{r^2} \quad (5b)$$

(Notice that even for large heat fluxes the intercept depends on the cylinder radius in contrast to the flat case).

6. Analysis of Ignition Data and discussion

We return now to the analysis of the experimental data in Figure 1. Because of unambiguous behavior, one should establish thermally thick conditions by using high heat fluxes or stacking samples tight. Thermally thick conditions can be obtained for thickness equal or greater than 2 mm and heat fluxes 50, 60 ,70 kW / m² (for additional comments see also ref.7).

A good procedure to utilize ignition data would be the following(refer to Figure 1 for evaluation):

1) For high heat fluxes and a plot of $t_{ign}^{-1.2}$ versus the applied heat flux \dot{q}'' , determine slope and intercept. Using Equ 3a, determine the critical heat flux from the intercept and the thermal resistance from the slope.

2) For heat fluxes near the critical heat flux ($< 1.5 \dot{q}_{cr}''$) find again the critical heat flux by extrapolation and compare with results in part 1. For “best” extrapolation plot t_{ign}^{-1} versus \dot{q}'' , because of the concave nature of the relation near the critical heat flux when one is using these variables (Equ. 2b and 3b).

Surface convective heat losses can be accounted for by replacing in all relations the definition of critical heat flux as

$$\dot{q}_{cr}'' = \sigma T_{ign}^4 + h_c (T_{ign} - T_o)$$

where h_c , the natural convective heat transfer coefficient over a horizontal surface, is about $5 \text{ W/m}^2 \text{ K}$.

REFERENCES

1. Scudamore M.J. et. al. “ Cone Calorimetry- A Review of Tests Carried out on Plastics for the Association of Plastic Manufacturers in Europe” Fire and Materials, 15, 65-84 , 1991.
2. Tewarson A., “ Generation of Heat and Chemical Compounds in Fires” SFPE Handbook. 2nd Edition, 3-53, 1995
3. Panagiotou et al., “ Ignition Times and Critical Heat Flux”, Combustion and Flame ,84,223,1991.
4. Chen Y. et al., “Material Pyrolysis Properties”, Combustion Science and Technology, 104,404-425,1995.
5. EPRI Report NP- 1767, 1981
6. Luikov . A. V. Analytical Heat diffusion Theory, Academic Press , 1968, pgs,178,194
7. Whitley, R.H. “ Some Comments on the Measurements of Ignitibility and on the Calculation of Critical Heat Flux” Fire Safety Journal , 21 , 177 –183, 1993

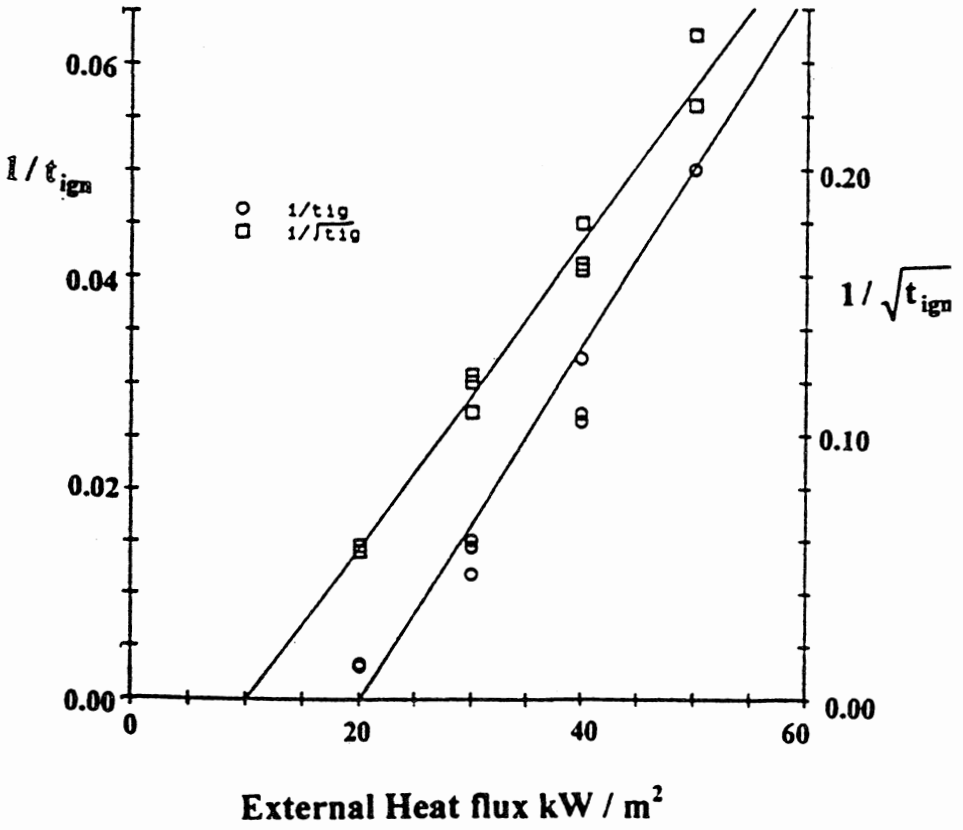


Figure 1. Ignition times [1] plotted as if thermally thick or thermally thin conditions prevail.

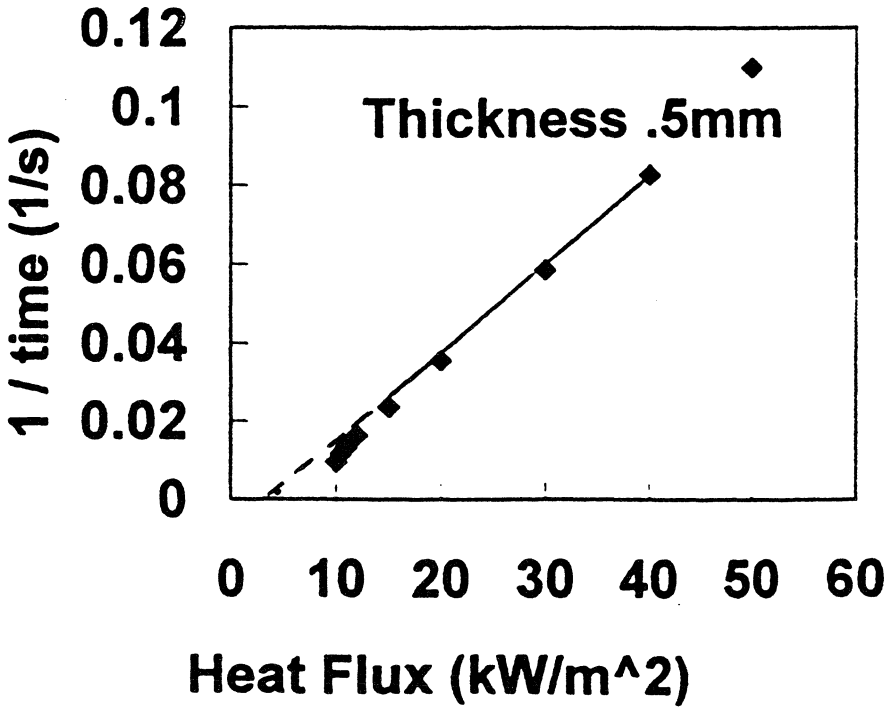


Figure 2. Numerical results for thermally thin conditions consistent with Eqs 2a and 2b.

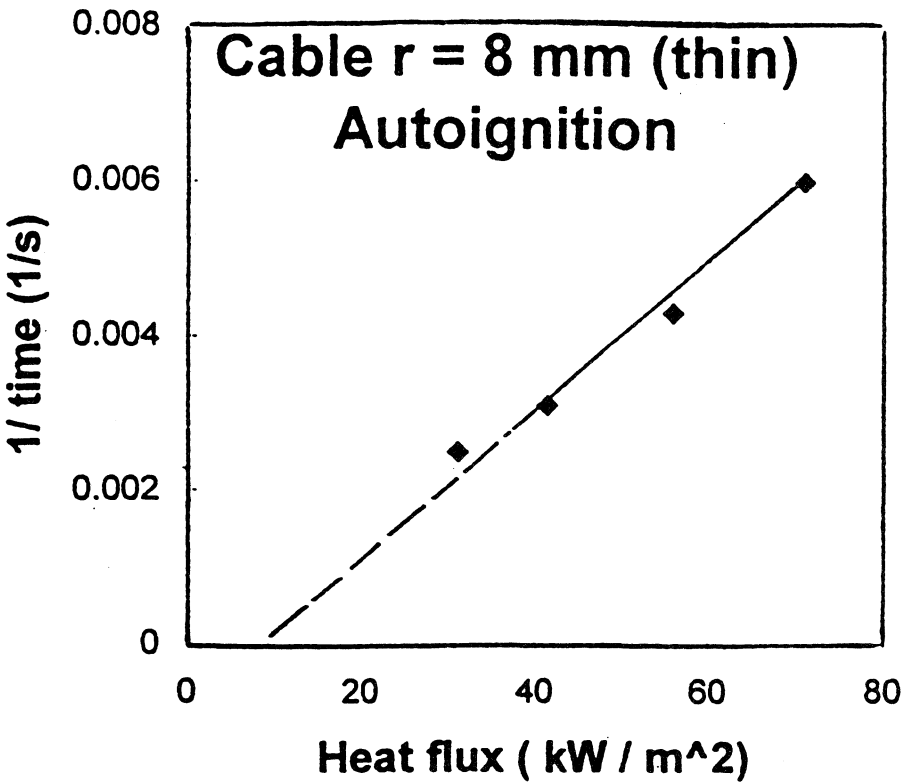


Figure 3. (Auto) Ignition times for a thermally thin cable showing that the intercept is about 1 / 3 of the critical heat flux(Equ 2a)

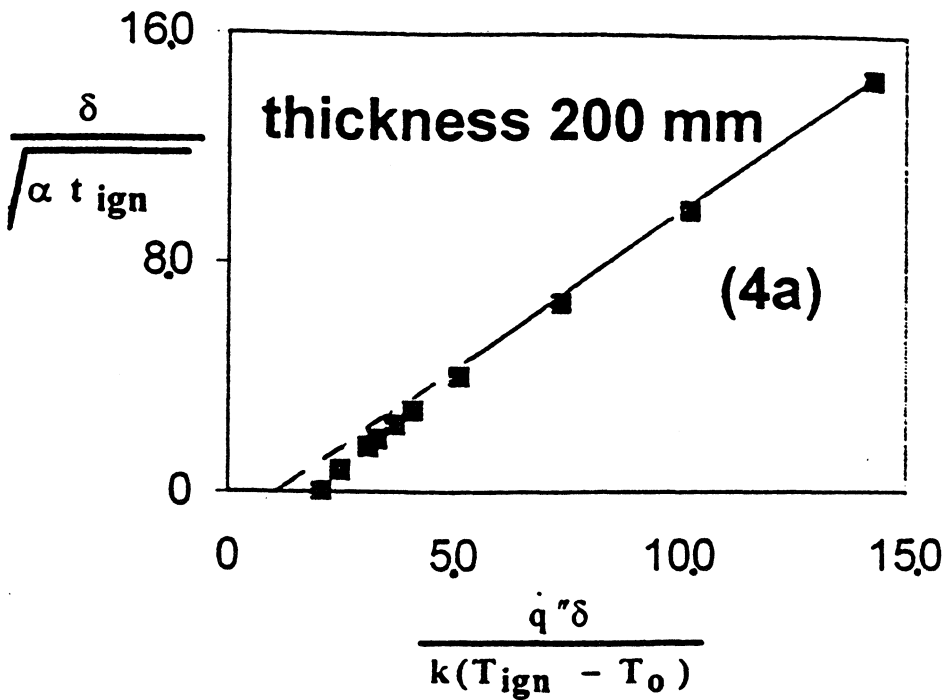


Figure 4. Numerical results for thermally thick to intermediate conditions :

(4a) for thickness 200 mm.

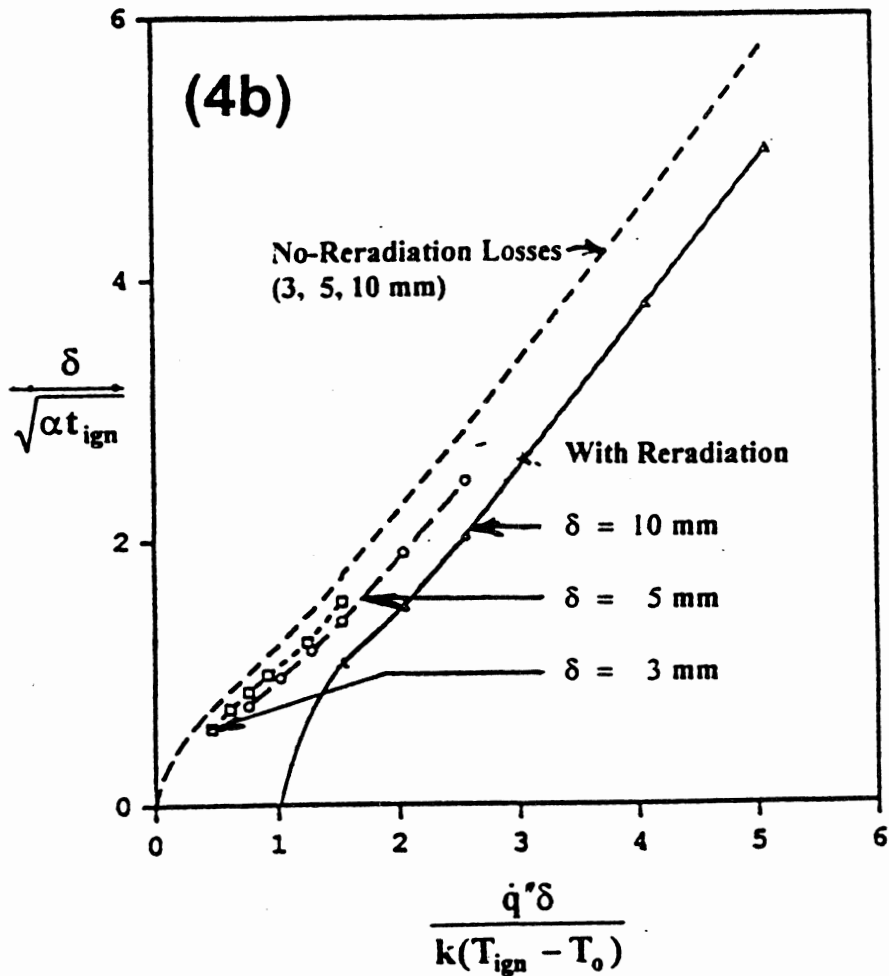


Figure 4. Numerical results for thermally thick to intermediate conditions :

(4b) without losses and with reradiation losses for thickness 3, 5, 10 mm

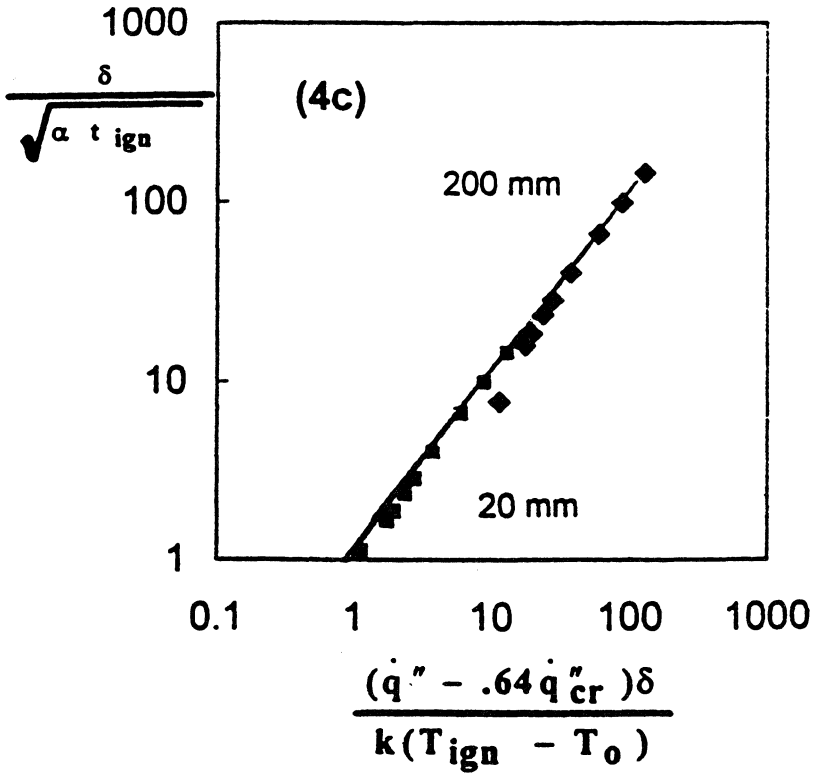


Figure 4. Numerical results for thermally thick to intermediate conditions :

**(4c) ignition data for 20 mm and 200 mm
accounting for the reduction of applied heat flux by $0.64 \dot{q}''_c$**

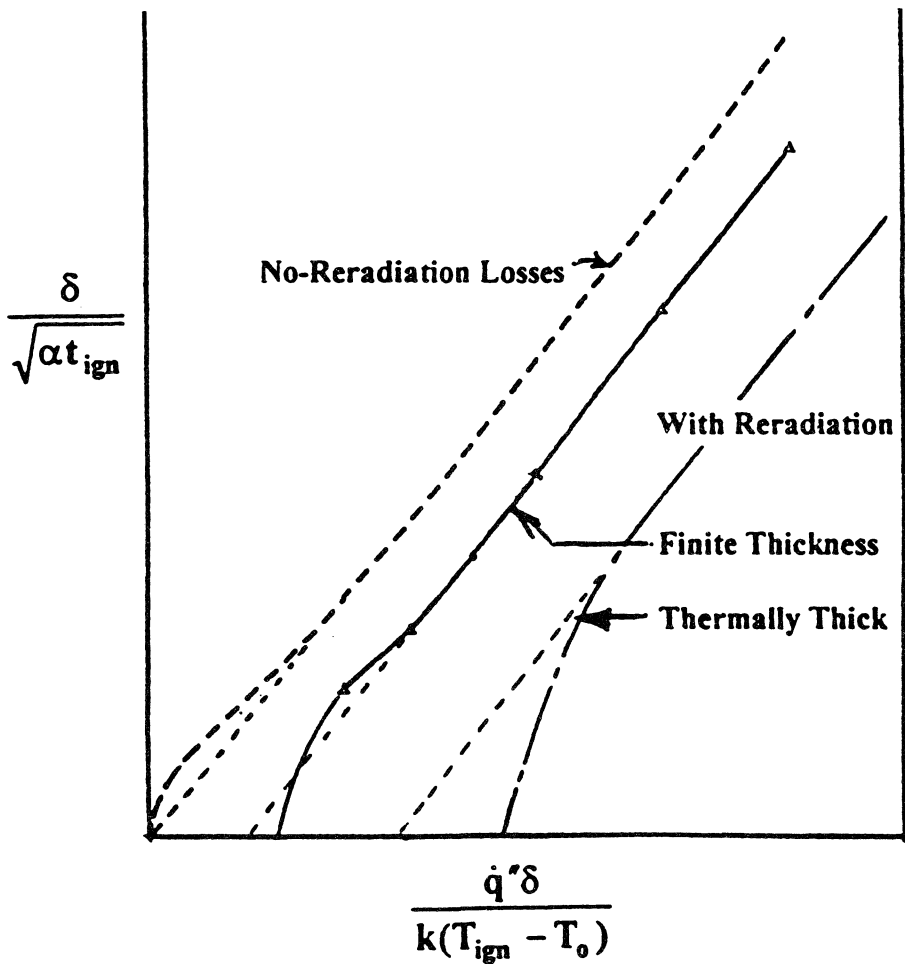


Figure 5. Qualitative illustration of the ignition time behavior at low heat fluxes.